Journal of Dental Research
2021, Vol. 100(4) 415–422

DOI: 10.1177/0022034520970459
journals.sagepub.com/home/jdr

Lrp6 Dynamic Expression in Tooth Development and Mutations in Oligodontia

M. Yu[1*], Z. Fan[1*], S.W. Wong[2], K. Sun[1], L. Zhang[1], H. Liu[1], H. Feng[1], Y. Liu[1], and D. Han[1]

Abstract

Genes associated with the WNT pathway play an important role in the etiology of tooth agenesis. Low-density lipoprotein receptor–related protein 6 encoding gene (*LRP6*) is a recently defined gene that is associated with autosomal dominant inherited tooth agenesis. Here, we aimed to identify novel *LRP6* mutations in patients with tooth agenesis and investigate the significance of *Lrp6* during tooth development. Using whole-exome sequencing, we identified 4 novel *LRP6* heterozygous mutations (c.2292G>A, c.195dup, c.1095dup, and c.1681C>T) in 4 of 77 oligodontia patients. Notably, a patient who carried a nonsense *LRP6* mutation (c.2292G>A; p.W764*) presented a hypohidrotic ectodermal dysplasia phenotype. Preliminary functional studies, including bioinformatics analysis and TOP-/FOP-flash reporter assays, demonstrated that the activation of WNT/β-catenin signaling was compromised as a consequence of *LRP6* mutations. RNAscope in situ hybridization revealed dynamic and special changes of *Lrp6* expression during murine tooth development from E11.5 to E16.5. It was noteworthy that *Lrp6* was specifically expressed in the epithelium at E11.5 to E13.5 but was expressed in both dental epithelium and dental papilla from E14.5 and persisted in both tissues at later stages. Our study broadens the mutation spectrum of human tooth agenesis and is the first to identify a *LRP6* mutation in patients with hypohidrotic ectodermal dysplasia and reveal the dynamic expression pattern of *Lrp6* during tooth development. Information from this study is conducive to understanding the functional significance of *Lrp6* on the biological process of tooth development.

Keywords: WNT signaling, genetics, pathogenicity, tooth abnormalities, odontogenesis, Low Density Lipoprotein Receptor-Related Protein-6

Introduction

With a prevalence varying from 0.03% to 10.2% among different areas and races, tooth agenesis is considered one of the most common craniofacial developmental defects in humans (Mattheeuws et al. 2004; Rakhshan and Rakhshan 2016). Hypodontia is the congenital absence of fewer than 6 permanent teeth, while permanent tooth agenesis of 6 or more teeth is defined as oligodontia (excluding the third molars). Oligodontia is even more rare, with an estimated incidence of 0.08% to 0.14% worldwide (Dhamo et al. 2018). Moreover, individuals with tooth agenesis often have morphological and structural abnormalities or eruption defects of the remaining teeth (Wong et al. 2018).

Genetic factors play a predominant role in the occurrence and pathogenesis of oligodontia and other dental development disorders (Yu, Wong, et al. 2019). Mutations in genes involved in the WNT/β-catenin, TGF-β/BMP, and EDA/EDAR/NF-κB pathways are responsible for the majority of oligodontia cases, including *WNT10A* (*wingless-type MMTV integration site family, member 10A*, 2q35; OMIM *606268), *WNT10B* (*wingless-type MMTV integration site family, member 10B*, 12q13.12; OMIM *601906), *AXIN2* (*axis inhibitor*, 17q24.1; OMIM *604025), *PAX9* (*paired box gene 9*, 14q13.3; OMIM *167416), *MSX1* (*Msh homeobox 1*, 4p16.2; OMIM *142983), *EDA* (*ectodysplasin A*, Xq13.1; OMIM *300451), *EDAR* (*ectodysplasin A receptor*, 2q13; OMIM *604095), and *EDARADD* (*EDAR-associated death domain*, 1q42-q43; OMIM *606603) (Han et al. 2008; van der Hout et al. 2008; Song et al. 2009; Bergendal

[1]Department of Prosthodontics, Peking University School and Hospital of Stomatology and National Clinical Research Center for Oral Diseases and National Engineering Laboratory for Digital and Material Technology of Stomatology and Beijing Key Laboratory of Digital Stomatology, Beijing, China
[2]Division of Comprehensive Oral Care–Periodontology, Adams School of Dentistry, University of North Carolina at Chapel Hill, Chapel Hill, NC, USA
*Authors contributing equally to this article.

A supplemental appendix to this article is available online.

Corresponding Authors:
D. Han, Department of Prosthodontics, Peking University School and Hospital of Stomatology and National Clinical Research Center for Oral Diseases and National Engineering Laboratory for Digital and Material Technology of Stomatology and Beijing Key Laboratory of Digital Stomatology, 22 Zhongguancun South Avenue, Beijing 100081, China.
Email: donghan@bjmu.edu.cn
Y. Liu, Department of Prosthodontics, Peking University School and Hospital of Stomatology and National Clinical Research Center for Oral Diseases and National Engineering Laboratory for Digital and Material Technology of Stomatology and Beijing Key Laboratory of Digital Stomatology, 22 Zhongguancun South Avenue, Beijing 100081, China.
Email: pkussliuyang@bjmu.edu.cn

et al. 2011; Song et al. 2014; Wong et al. 2014; Yu et al. 2016; Bonczek et al. 2018; Wong et al. 2018; Yu, Liu, et al. 2019).

The WNT pathway plays a crucial role in regulating cell differentiation, cell proliferation, and cell migration during dental and orofacial development (Thesleff and Sharpe 1997; Li et al. 2017). Low-density lipoprotein receptor–related protein 6 (LRP6, OMIM *603507), a single-pass transmembrane receptor, is a member of the low-density lipoprotein (LDL) receptor–related proteins family and functions as a vital coreceptor for WNTs (MacDonald and He, 2012). LRP6 has 1 extracellular domain consisting of 4 β-propellers and neighboring EGF-like repeats (E1–4), followed by 3 low-density lipoprotein receptor (LDLR) type A repeats. Moreover, a recent study reported that the LRP6 binding sites for WNT ligands or other inhibitors, such as SOST and DKK1, are located at the surface of its E1 to E3 functional domains (MacDonald and He 2012; Joiner et al. 2013).

To date, *LRP6* has been associated with a broad panel of human diseases, such as late-onset Alzheimer disease (De Ferrari et al. 2007), osteoporosis (Williams and Insogna 2009), coronary artery disease alongside with atherosclerosis, and some metabolic syndromes, including diabetes, hypertension, and hyperlipidemia (Mani et al. 2007; Singh et al. 2013; Xu et al. 2014), spina bifida (Lei et al. 2015), neural tube defects (Shi et al. 2018), and prostate cancer (Roslan et al. 2019). Recently, *LRP6* was reported as a novel candidate gene in nonsyndromic oligodontia (Massink et al. 2015), which further highlighted the etiological significance of the WNT pathway in human tooth agenesis (Yu, Wong, et al. 2019). Mutations in the *LRP6* gene were also identified in cleft lip and/or palate, as well as tooth agenesis with minor anatomical congenital defects of the fingers and the ear (Ockeloen et al. 2016; Basha et al. 2018; Dinckan et al. 2018; Ross et al. 2019). Despite the important role of LRP6 during tooth development, the expression pattern of *LRP6* has never been investigated.

In this study, we identified 4 novel *LRP6* mutations, including 2 nonsense (c.2292G>A and c.1681C>T) and 2 frameshift (c.195dup and c.1095dup) mutations in 4 of the 77 patients with oligodontia. Tertiary structural and in vitro functional analysis revealed that the activation of WNT/β-catenin signaling was severely impaired by loss of function of LRP6. Our findings confirm that *LRP6* is the pathogenic gene for oligodontia. Importantly, we also defined the dynamic expression pattern of *Lrp6* at serial tooth developmental stages in mice, implicating its role in tooth development.

Materials and Methods

Participant Recruitment

A cohort of 77 participants with oligodontia was recruited from the Department of Prosthodontics at Peking University School and Hospital of Stomatology, Beijing, China. All participants denied a history of tooth extraction or loss, confirming the nature of congenital tooth missing. Informed consent was signed by all participants. Detailed intraoral and radiographic examinations were performed by a prosthodontist. All experiments were approved by the Ethics Committee of Peking University School and Hospital of Stomatology (PKUSSIRB-201736082) and the Institutional Animal Care and Use Committees at the Peking University Health Science Center (LA2016078).

Whole-Exome Sequencing Analysis

Genomic DNA of each proband were extracted from peripheral blood lymphocytes using the Blood Genomic DNA Mini-Kit (Cwbiotech) and sent for whole-exome sequencing (WES) with the Illumina-X10 platform by iGeneTech. To filter the detected variants, orodental-related genes were annotated (Prasad et al. 2016). Then, we excluded silent variants and missense variants with a minor allele frequency (MAF) ≥0.01 in East Asians in the single Nucleotide Polymorphism database (dbSNP), the 1000 Genomes Project database (1000G), the Genome Aggregation Database (gnomAD), or the Exome Aggregation Consortium (ExAC). Sorting Intolerant from Tolerant (SIFT), Polymorphism Phenotyping v2 (PolyPhen-2), and Mutation Taster were carried out for the bioinformatic analysis to predict the functional impact of the remaining variants.

We confirmed 4 novel pathogenic variants of the *LRP6* (NM_002336.3) and excluded other candidate genes in 4 affected families. Cosegregation analysis and Sanger sequencing (primers are in Appendix Table 1) of the probands and their family members were employed to validate *LRP6* variants in the family pedigrees. TA clone sequencing was used to confirm the frameshift mutations.

Tertiary Structural Modeling and Conformational Analysis

The crystal structure of the 4 β-propeller–EGF fragments in LRP6: LRP6-E1E2 (Protein Data Bank database, PDB database ID, 5gje.1.A) and LRP6-E3E4 (PDB database ID, 6h15.1.A) (Cheng et al. 2011) was used as a template to predict the conformational effect of the *LRP6* mutations. Visualization of the tertiary structure of wild-type and mutant LRP6 proteins was drawn using the PyMOL2.3 Molecular Graphics System.

LRP6 Plasmid Generation

To generate a wild-type *LRP6* plasmid, the full-length coding sequence of the human *LRP6* gene was subcloned into an empty pEGFP-M98 vector between 5′-NspV and 3′-XhoI. Y66Ifs*4, D366Rfs*13, R561*, and W764* were designed as previously described (Lee et al. 2010). Primers are in Appendix Table 1. TOP-flash (a TCF reporter plasmid) and FOP-flash (a mutant TCF reporter plasmid) were obtained from MiaoLing Plasmid (Miaoling Bioscience).

Western Blot Analysis

Human embryonic kidney 293T (HEK-293T) cells were transfected with the empty vector, the wild-type and mutant LRP6

plasmids using Lipofectamine 3000 (Invitrogen). Then, 40 µg of total protein was extracted from the transfected cells and 80 µg of secretory protein was extracted from their culture supernatant fluids using the Cultural Supernatants Total Protein Extraction Kit (applygen). Protein lysates were resolved by sodium dodecyl sulfate–polyacrylamide gel electrophoresis (SDS-PAGE) and transferred onto a nitrocellulose membrane. Blots were probed with anti-GFP (Abcam) and anti-GAPDH (Sungene Biotech) antibodies.

TOP-/FOP-Flash Reporter Assay

Equivalent amounts (1.5 µg) of each construct alone (empty vector, wild type, and mutant) or coexpression of wild type (0.75 µg) and each mutant (0.75 µg) were cotransfected with either a TOP-flash or FOP-flash reporter plasmid into HEK-293T cells. The phRL-TK (*Renilla* reporter plasmid; Promega) was used as an endogenous reference. Twenty-four hours after transfection, cells were cultured in the absence or presence of 100 ng/mL Wnt3a (R&D) for 8 h, respectively. Cell lysates were used to measure both firefly and *Renilla* luciferase activity in replicates by a dual-luciferase reporter system (Promega). Firefly luciferase activity was normalized to the *Renilla* luciferase for each sample. The Wnt/β-catenin activation was determined as the ratio of TOP-/FOP-luciferase activity with or without Wnt3a stimulated. Student's *t* test was carried out to compare the difference of relative activity between the wild type and mutants. Data were presented as mean ± SD ($n=3$), and $P<0.001$ was considered statistically significant.

Tooth Germ Preparation and RNAscope In Situ RNA Analysis

According to the appearance of a vaginal plug, timed-pregnant ICR mice were sacrificed at the stages of embryonic (E) day 11.5 (E11.5), E12.5, E13.5, E14.5, E15.5, and E16.5, respectively. Three embryonic heads of each developmental stage were microdissected and fixed in 4% paraformaldehyde for 24 h and ethanol series dehydrated, paraffin embedded, and serially sectioned (5 µm) in the coronal plane. RNAscope Probe-Mm-Lrp6 (Advanced Cell Diagnostics; ACD, 315801) and Probe-Mm-Lrp5 (ACD, 315791) were designed to target the 2097 to 2992 bp of mouse *Lrp6* messenger RNA (mRNA) (NM_008514.4) and the 1261 to 2246 bp of mouse *Lrp5* mRNA (NM_008513.3), respectively. RNAscope 2.5 HD detection reagents–RED analysis system (ACD, 322360) was used to explore the expression pattern of *Lrp6* and *Lrp5* following the manufacturer's protocol (Wang et al. 2012).

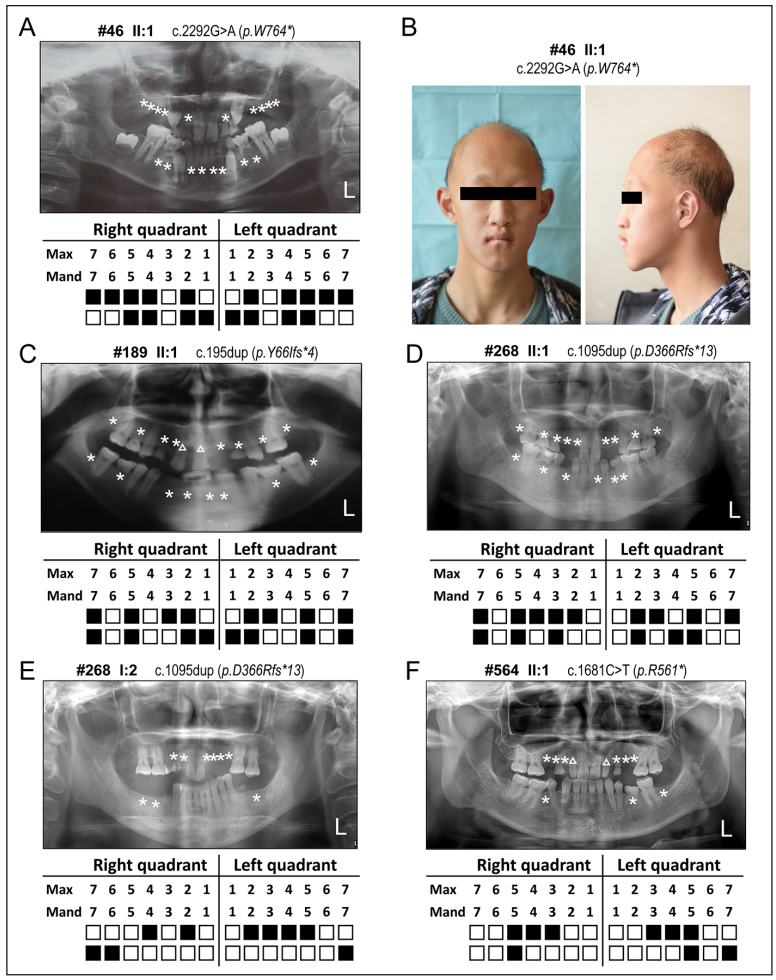

Figure 1. Clinical features of patients with tooth agenesis. (**A**) Panoramic radiograph and schematic of #46 proband (II:1) with congenital lack of permanent teeth. (**B**) Facial photographs of #46 II:1 showing sparse hair and eyebrows. (**C**) Panoramic radiograph and schematic of #189 proband (II:1) with congenital missing permanent teeth. (**D**, **E**) Panoramic radiograph and schematic of #268 (II:1) proband with congenital missing permanent teeth and the mother of the proband (I:2). (**F**) Panoramic radiograph and schematic of #564 proband (II:1) with congenital missing permanent teeth. Asterisks in panoramic radiographs and solid squares in the schematics indicate congenital missing permanent teeth. Triangles in panoramic radiographs indicate cone-shaped teeth. L, left; Mand, mandibular; Max, maxillary.

Results

Clinical Examination and Variants Identification

Four novel *LRP6* heterozygous mutations (c.2292G>A, c.195dup, c.1095dup, and c.1681C>T) were identified in 4 of 77 oligodontia patients, with a mutation detection rate of 5.2% (4/77).

An 11-y-old male proband (II:1) of family #46 had 18 congenital missing permanent teeth (Fig. 1A). This proband showed hypohidrotic ectodermal dysplasia-associated features, such as sparse hair and hypohidrosis (Fig. 1B). WES screening revealed a heterozygous nonsense mutation c.2292G>A (p.W764*) in exon 11 of the *LRP6* gene in the proband (Fig. 2A). There was no pathogenic mutation identified in

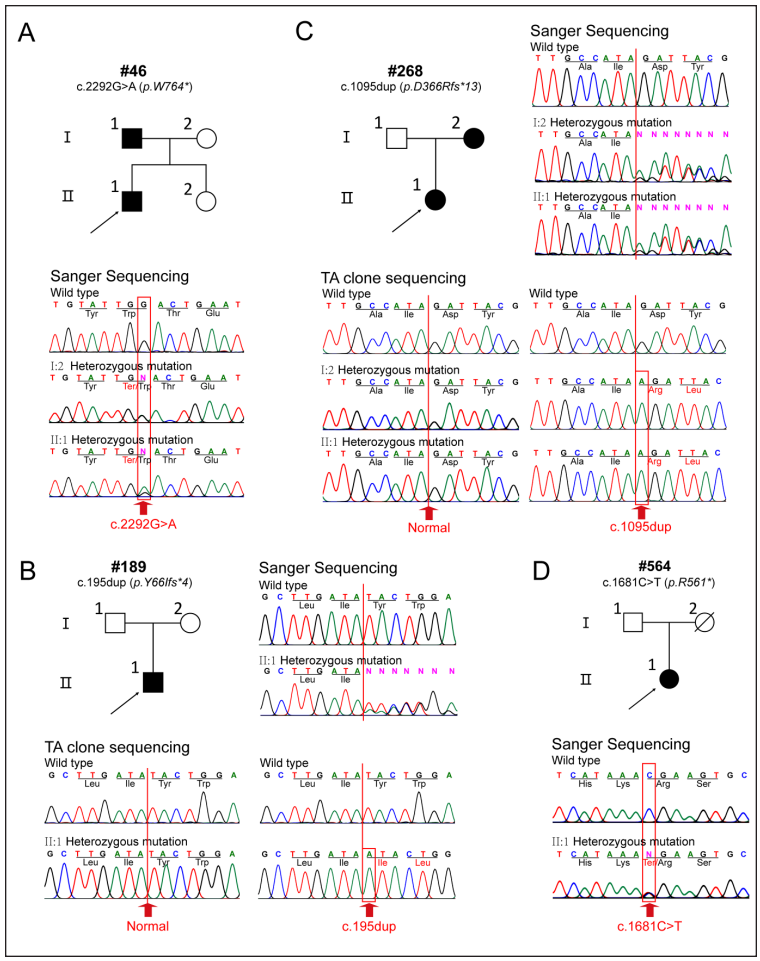

Figure 2. Pedigrees in tooth agenesis patients and genetic screen of *LRP6* mutations. (**A**) Sequencing chromatograms show a heterozygous *LRP6* nonsense mutation (c.2292G>A; p.W764*) identified in #46 II:1 and #46 I:1. (**B**) Sequencing chromatograms show a heterozygous *LRP6* frameshift mutation (c.195dup; Y66Ifs*4) identified in #189 II:1. (**C**) Sequencing chromatograms show a heterozygous *LRP6* frameshift mutation (c.1095dup; p.D366Rfs*13) identified in #268 II:1 and #268 I:2. (**D**) Sequencing chromatograms show a heterozygous *LRP6* nonsense mutation (c.1681C>T; p.R561*) identified in #564 II:1. Black arrows indicate the proband in each family. Solid circles and squares represent the individuals with tooth agenesis. All mutated nucleotides are labeled with red frames and red arrows.

ectodermal dysplasia-related genes, such as the genes of the *EDA* pathway (Appendix Table 2). The proband's father exhibited nonsyndromic oligodontia, with normal characteristics of the hair and sweat glands, and also carried the heterozygous *LRP6* mutation c.2292G>A. This mutation was not detected in his unaffected mother or sister. Therefore, the proband's *LPR6* mutation c.2292G>A (p.W764*) was inherited from his father and cosegregated with oligodontia in a dominant manner (Fig. 2A).

A 19-y-old male proband (II:1) of family #189 was diagnosed with congenitally missing 16 permanent teeth, and he also had cone-shaped maxillary central incisors (Fig. 1C). His facial features, hair, sweat, and skin were normal. The dentitions and other ectodermal organs of his parents were unaffected, and the patient denied a family history of tooth agenesis or ectodermal abnormalities. A heterozygous frameshift mutation c.195dup (p.Y66Ifs*4) located in exon 2 of the *LRP6* gene was detected in the proband (Fig. 2B). However, this mutation was not detected in his asymptomatic parents, suggesting that the proband's *LRP6* mutation c.272_273insA (p.Y66Ifs*4) was a novel de novo mutation (Fig. 2B).

The proband (II:1) of family #268 was a 20-y-old female who presented with the absence of 15 permanent teeth (Fig. 1D). Her mother (I:2) also had 7 permanent teeth congenitally missing (Fig. 1E), but her father was not affected. No obvious systemic anomaly was observed in this family. A heterozygous frameshift mutation c.1095dup (p.D366Rfs*13) in exon 6 of the *LRP6* gene was detected in the proband and her mother, indicating that the proband's *LRP6* mutation was inherited from her mother (Fig. 2C).

In family #564, a 21-y-old female proband (II:1) had 9 permanent teeth missing and cone-shaped maxillary lateral incisors (Fig. 1F). Her father was unaffected with tooth agenesis or other systemic anomalies while her mother's clinical manifestation and genotype were unavailable because of her death. A heterozygous nonsense mutation c.1681C>T (p.R561*) in exon 8 of the *LRP6* gene was detected in the proband (Fig. 2D).

Conformational Changes of LRP6 Mutants

The extracellular domain of wild-type LRP6 consists of 4 continuous "YWTD-β-propeller-EGF-like" domains: E1 to E4 domains (Cheng et al. 2011), which are presented in Figure 3A, B, D, F, and H. When compared with wild-type LRP6 conformation, the p.W764* mutation located at the E3 domain led to a premature termination at residue Trp764 (Fig. 3B, C). The p.Y66Ifs*4 mutation was located at the E1 domain of LRP6 and resulted in a frameshift from residue 66 to the resultant premature stop at residue 70. The conformation of the helix and sheet, adjacent to residue 70, was converted into a loop in this LRP6 mutant (Fig. 3D, E). The p.D366Rfs*13 mutation at the E2 domain also caused a premature truncation at residue 379 and a more marked conformational change near residue 379. Two sheets in this site converted into loops (Fig. 3F, G). For the p.R561* mutant, a premature truncation occurred at residue 561, which only left the signal peptide, E1, and partial E2 domains intact (Fig. 3H, I). Therefore, these diverse conformational changes of LRP6 mutants suggested that these 4 novel mutations may affect the biological functions of LRP6.

Expression of the LRP6 Mutants

We next accessed the functional consequences of LRP6 mutants by overexpressing wild-type or mutant LRP6 in HEK-293T cells. Western blot analysis showed that all 4 mutant proteins

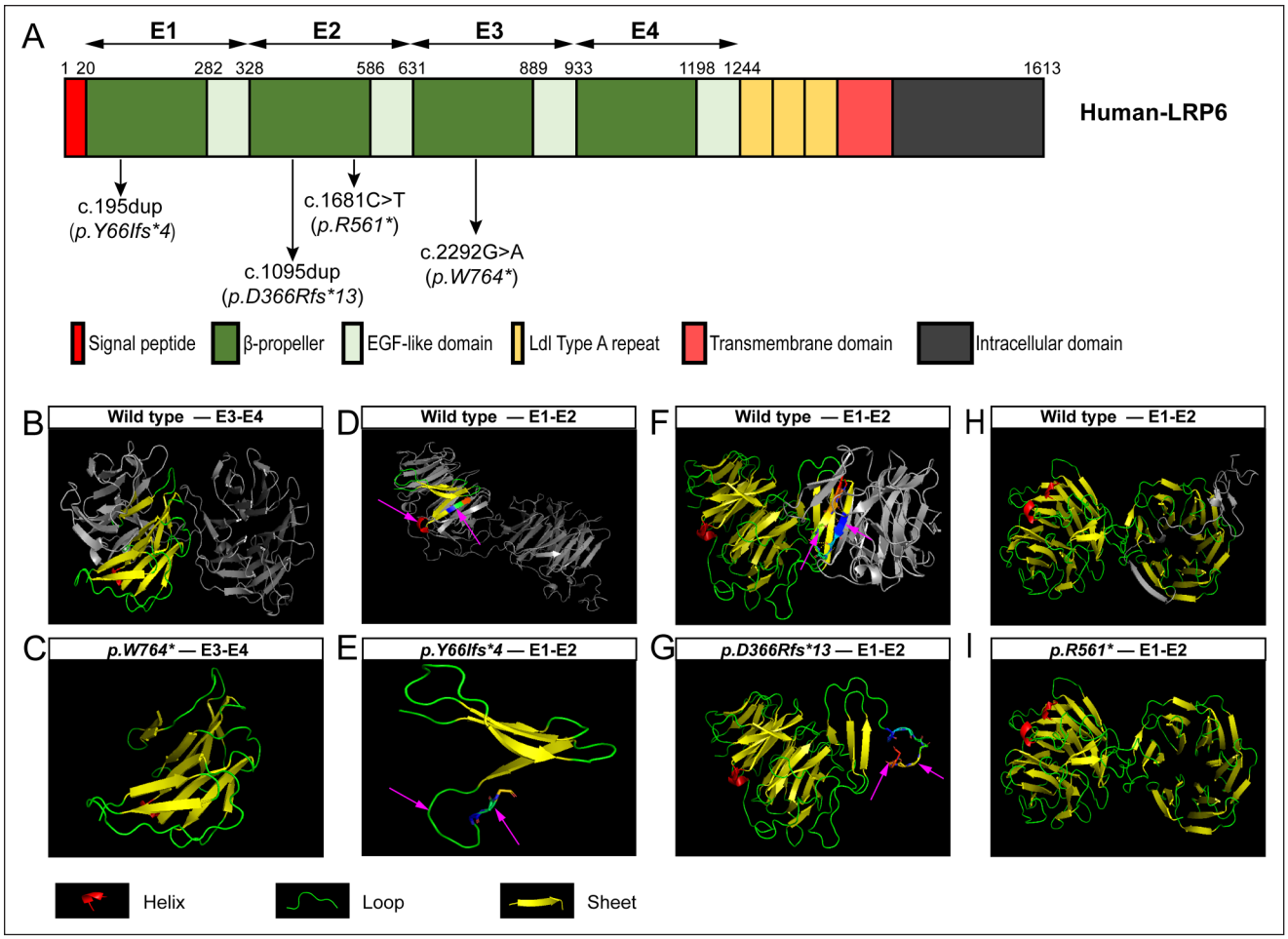

Figure 3. Location and tertiary structural analysis of LRP6 mutants. (**A**) Schematic diagram of the wild-type human LRP6 (NP_002327.2) protein and the distribution of the 4 novel LRP6 mutations identified in patients with tooth agenesis. E1 to E4 represent the 4 β-propeller–EGF–like repeats in the extracellular domain of LRP6. (**B–I**) Structural changes of 4 mutant LRP6 proteins (C, E, G, and I) compared with the wild-type E1–E2 and E3–E4 of LRP6 (B, D, F, and H).

with a GFP-tag could be expressed in vitro. The wild-type and the truncated LRP6 proteins (p.Y66Ifs*4, p.D366Rfs*13, p.R561*, and p.W764*) were produced at the predicted molecular weight (Fig. 4A). Since all truncated LRP6 proteins lacked the transmembrane domain, we next assessed if these mutants could be secreted in the culture media of transfected cells. Intriguingly, these truncated LRP6 were not detectable in the culture supernatant media (Appendix Fig.).

LRP6 Mutants Inhibit WNT/β-Catenin Signaling Activation through a Dominant-Negative Behavior

The TOP-/FOP-flash activities results showed that the TOP-/FOP-flash luciferase activity of Wnt3a was significantly lower in HEK-293T cells transfected with 4 LRP6 mutant plasmids when compared to those transfected with wild-type plasmids ($P<0.001$; Fig. 4B), indicating that 4 LRP6 mutants severely reduced WNT/β-catenin signaling activities. To investigate the mechanism of dominant-negative effect, we coexpressed wild-type LRP6 with each truncated mutant and then observed that all the 4 truncated mutants were able to suppress the activity of TOP-/FOP-flash luciferase stimulated by wild-type LRP6 (Fig. 4B).

Dynamic Expression Pattern of Lrp6 during Mouse Molar Development

These results demonstrated the loss-of-function LRP6 mutations in human oligodontia patients, suggesting an important role of LRP6 in regulating dental organogenesis. The expression pattern of *Lrp6* during tooth development, however, is hitherto unknown. To corroborate the role of *Lrp6* in tooth development, we performed an RNAscope assay to visualize the spatial and temporal expressions of *Lrp6* and its homolog, *Lrp5*, on mouse first mandibular molars at serial developmental stages. We found that the expression pattern of *Lrp6* exhibited dynamic changes from E11.5 to E16.5. At E11.5, when the ectoderm-derived dental epithelium thickened to form the dental lamina, the expression of *Lrp6* was detected in the dental lamina and the surrounding cranial neural crest–derived mesenchyme, which gave rise to mandible (Fig. 5A). At E12.5 to

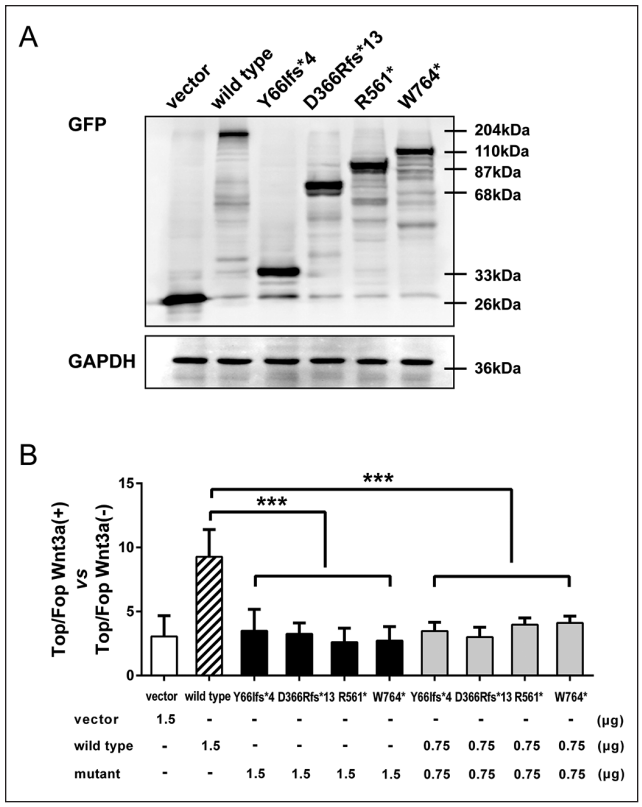

Figure 4. Expression and TOP-/FOP-flash luciferase reporter assay of LRP6 mutants. (**A**) Western blot analysis of wild-type and LRP6 mutants. An empty vector was transfected into cells as a negative control. (**B**) The TOP-/FOP-flash luciferase assay shows the transcriptional activation of the WNT/β-catenin signaling pathway in wild-type and mutant groups. The asterisks denote the difference with statistical significance (***$P < 0.001$), and the results are depicted as mean ± SD of triplicate experiments.

E13.5 (the bud stage), when the dental mesenchyme began to develop and surround the epithelial bud, the expression of *Lrp6* was restricted to the dental epithelium but was hardly detected in the dental mesenchyme (Fig. 5B, C). Strikingly, at E14.5 (the cap stage), *Lrp6* was expressed not only in the dental epithelium, including the primary enamel knot (EK) and the inner and outer enamel epithelium (IEE and OEE), but also in the dental papilla (Fig. 5G). Later, at the bell stage (E15.5–E16.5), *Lrp6* was highly expressed in the dental papilla and moderately expressed in the IEE and OEE (Fig. 5H, I). It is noteworthy that *Lrp6* expression was never detected in the dental follicle from E14.5 to E16.5. Furthermore, our results demonstrated that the expression pattern of *Lrp5* was highly consistent with that of *Lrp6* in the tooth germs of E11.5 to E16.5 mouse embryos (Fig. 5D–F, J–L).

Discussion

Although *LRP6* mutations have been previously identified in tooth agenesis (Appendix Table 3), novel mutations need to be continually discovered to broaden the genotypic and phenotypic spectrum associated with *LRP6* mutations. Here, we identified 4 novel *LRP6* pathogenic mutations in 4 unrelated oligodontia families, including 2 frameshift mutations (c.195 dup; p.Y66Ifs*4, c.1095dup; p.D366Rfs*13) and 2 nonsense mutations (c.1681C>T; p.R561*, c.2292G>A; p.W764*). Interestingly, we observed a notable phenotypic variation within a *LRP6*-related tooth agenesis family. A patient who carried a nonsense *LRP6* mutation (c.2292G>A; p.W764*) had a hypohidrotic ectodermal dysplasia phenotype, including sparse scalp hair, hypohidrosis, and oligodontia, while his father who carried the same mutation only showed nonsyndromic tooth agenesis. The phenotypic heterogeneity of *LRP6* mutations may due to an incomplete penetrance of the phenotype. Other possible factors, such as genetic and epigenetic modifiers, may also be implicated in the pathogenesis of hypohidrotic ectodermal dysplasia and tooth agenesis.

Physiologically, LRP6 forms a complex with WNTs and Frizzled (FZD) to activate the WNT signaling pathway. Consequently, newly synthesized β-catenin translocates into the nucleus and binds to members of the lymphoid enhancer binding factor (LEF)/T cell–specific transcription factor (TCF) family of transcription factors, thereby facilitating the transcription of WNT target genes (Logan and Nusse 2004). Variations in LEF/TCF transcription that decrease the activation of WNT target genes can lead to abnormalities in tooth development (van Genderen et al. 1994). Our tertiary structural analysis revealed that 3 LDLR type A domains, the transmembrane domain, and the intracellular domain of LRP6 were all disrupted by various degrees in the mutants, which may affect the WNT signaling activations as a consequence.

Indeed, in vitro experiment results demonstrated that these truncated LRP6 proteins compromised canonical WNT activations. To further mimic the heterozygosity found in the affected patients, an equivalent amount of wild-type and mutant *LRP6* plasmids was cotransfected into the cells, and the results indicated that p.Y66Ifs*4, p.D366Rfs*13, p.R561*, and p.W764* mutations might have a dominant-negative effect on the activity of the wild-type allele in regulating WNT activations, contributing to oligodontia pathogenesis.

LRP5 shares 73% sequence identity with LRP6 in the extracellular domain and 64% in the intercellular domain (Roslan et al. 2019). During embryonic development, LRP5 is a collaborative factor with LRP6, forming a trimeric complex (WNT–FZD–LRP5/6) together with WNT receptors and FZD, which then activates the WNT/β-catenin signaling pathway (Roslan et al. 2019). Since the WNT/β-catenin signaling pathway plays a vital role in the process of tooth development (Liu and Millar 2010), we speculated that *Lrp6*, possibly together with *Lrp5*, is involved in controlling tooth development. We analyzed the expression patterns of *Lrp6* and *Lrp5* at serial stages of mouse tooth germ development by RNAscope analysis. Interestingly, we found that the expression pattern of *Lrp6* exhibits dynamic changes, and the expression patterns of *Lrp6* and *Lrp5* transcripts are highly overlapping in the tooth germs of E11.5 to E16.5 mouse embryos. *Lrp6* and *Lrp5* were specifically expressed in the dental epithelium at E11.5 to E13.5. It is noteworthy that the expression of *Lrp6* and *Lrp5* was first detected in both dental papilla and dental epithelium from

E14.5 and persisted in both tissues at later stages. These data may indicate the crucial roles of *Lrp6* and *Lrp5* in regulating epithelial-mesenchymal interactions during tooth development. However, *Lrp6* and *Lrp5* transcripts were never expressed in the dental follicle of E14.5 to E16.5 mouse embryos, suggesting that the development of dental follicle–derived tissues, such as cementum and periodontal membrane, are Lrp6/5 independent.

Mutations in *WNT10A* and *WNT10B* also lead to oligodontia and share a similar localization pattern in the dental epithelium at the bud and cap stages, when tooth morphogenesis is first apparent (Yu et al. 2016). From E15.5 to the later stage, *Wnt10b* is exclusively expressed in the dental epithelium (Dassule et al. 1998), while *Wnt10a* expression is gradually detected in both the dental epithelium and adjacent mesenchyme (Yu et al. 2020). The partially overlapped expression patterns of the WNT ligands, *Wnt10a* and *Wnt10b*, with the WNT coreceptors, *Lrp6* and *Lrp5*, indicate the precise regulation networks of Wnt/β-catenin signaling in tooth development.

Taken together, we reported 4 novel *LRP6* mutations in oligodontia patients, and our results greatly expand the mutation spectrum of human tooth agenesis. Our data provide in vivo evidence that *Lrp6* and *Lrp5* may play crucial roles in epithelial-mesenchymal interactions during tooth morphogenesis. The precise regulatory mechanisms of *Lrp6* and *Lrp5* in tooth development need to be further investigated by constructing gene conditional knockout mouse models.

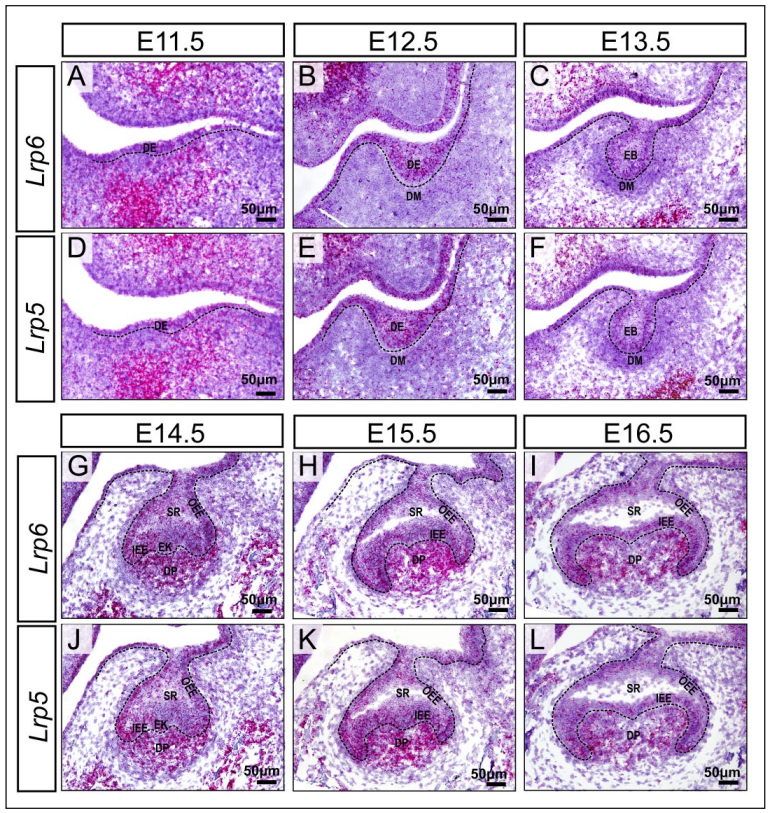

Figure 5. Expression patterns of *Lrp6* and *Lrp5* during early tooth development in mouse. The expression patterns of *Lrp6* (**A–C**) and *Lrp5* (**D–F**) detected by RNAscope assay from the dental epithelium thickening stage (E11.5) to the bud stage (E13.5). The expression patterns of *Lrp6* (**G–I**) and *Lrp5* (**J–L**) detected by RNAscope assay from the cap stage (E14.5) to the bell stage (E16.5). DE, dental epithelium; DM, dental mesenchyme; DP, dental papilla; EB, epithelial bud; EK, enamel knot; IEE, inner enamel epithelium; OEE, outer enamel epithelium; SR, stellate reticulum. Scale bars: 50 μm.

Author Contributions

M. Yu, contributed to data acquisition, analysis, and interpretation, drafted and critically revised the manuscript; Z. Fan, contributed to data acquisition, analysis, and interpretation, drafted the manuscript; S.W. Wong, H. Feng, Y. Liu, D. Han, contributed to conception and design, critically revised the manuscript; K. Sun, L. Zhang, H. Liu, contributed to data acquisition, drafted the manuscript. All authors gave final approval and agree to be accountable for all aspects of the work.

Acknowledgments

We thank the patients and their families for their participation in the study.

Declaration of Conflicting Interests

The authors declared no potential conflicts of interest with respect to the research, authorship, and/or publication of this article.

Funding

The authors disclosed receipt of the following financial support for the research, authorship, and/or publication of this article: This work was supported by the National Natural Science Foundation of China (81970902, 81771054, and 81600846).

ORCID iD

D. Han https://orcid.org/0000-0001-9625-3384

References

Basha M, Demeer B, Revencu N, Helaers R, Theys S, Bou Saba S, Boute O, Devauchelle B, Francois G, Bayet B, et al. 2018. Whole exome sequencing identifies mutations in 10% of patients with familial non-syndromic cleft lip and/or palate in genes mutated in well-known syndromes. J Med Genet. 55(7):449–458.

Bergendal B, Klar J, Stecksen-Blicks C, Norderyd J, Dahl N. 2011. Isolated oligodontia associated with mutations in EDARADD, AXIN2, MSX1, and PAX9 genes. Am J Med Genet A. 155A(7):1616–1622.

Bonczek O, Bielik P, Krejci P, Zeman T, Izakovicova-Holla L, Soukalova J, Vanek J, Gerguri T, Balcar VJ, Sery O. 2018. Next generation sequencing reveals a novel nonsense mutation in msx1 gene related to oligodontia. PLoS One. 13(9):e0202989.

Cheng Z, Biechele T, Wei Z, Morrone S, Moon RT, Wang L, Xu W. 2011. Crystal structures of the extracellular domain of LRP6 and its complex with DKK1. Nat Struct Mol Biol. 18(11):1204–1210.

Dassule HR, McMahon AP. 1998. Analysis of epithelial-mesenchymal interactions in the initial morphogenesis of the mammalian tooth. Dev Biol. 202(2):215–227.

De Ferrari GV, Papassotiropoulos A, Biechele T, Wavrant De-Vrieze F, Avila ME, Major MB, Myers A, Saez K, Henriquez JP, Zhao A, et al. 2007. Common genetic variation within the low-density lipoprotein receptor-related protein 6 and late-onset Alzheimer's disease. Proc Natl Acad Sci U S A. 104(22):9434–9439.

Dhamo B, Kuijpers MAR, Balk-Leurs I, Boxum C, Wolvius EB, Ongkosuwito EM. 2018. Disturbances of dental development distinguish patients with oligodontia-ectodermal dysplasia from isolated oligodontia. Orthod Craniofac Res. 21(1):48–56.

Dinckan N, Du R, Petty LE, Coban-Akdemir Z, Jhangiani SN, Paine I, Baugh EH, Erdem AP, Kayserili H, Doddapaneni H, et al. 2018. Whole-exome sequencing identifies novel variants for tooth agenesis. J Dent Res. 97(1):49–59.

Han D, Gong Y, Wu H, Zhang X, Yan M, Wang X, Qu H, Feng H, Song S. 2008. Novel EDA mutation resulting in X-linked non-syndromic hypodontia and the pattern of EDA-associated isolated tooth agenesis. Eur J Med Genet. 51(6):536–546.

Joiner DM, Ke J, Zhong Z, Xu HE, Williams BO. 2013. LRP5 and LRP6 in development and disease. Trends Endocrinol Metab. 24(1):31–39.

Lee J, Shin MK, Ryu DK, Kim S, Ryu WS. 2010. Insertion and deletion mutagenesis by overlap extension PCR. Methods Mol Biol. 634:137–146.

Lei Y, Fathe K, McCartney D, Zhu H, Yang W, Ross ME, Shaw GM, Finnell RH. 2015. Rare LRP6 variants identified in spina bifida patients. Hum Mutat. 36(3):342–349.

Li J, Parada C, Chai Y. 2017. Cellular and molecular mechanisms of tooth root development. Development. 144(3):374–384.

Liu F, Millar SE. 2010. WNT/β-catenin signaling in oral tissue development and disease. J Dent Res. 89(4):318–330.

Logan CY, Nusse R. 2004. The wnt signaling pathway in development and disease. Annu Rev Cell Dev Biol. 20:781–810.

MacDonald BT, He X. 2012. Frizzled and LRP5/6 receptors for wnt/beta-catenin signaling. Cold Spring Harb Perspect Biol. 4(12):a007880.

Mani A, Radhakrishnan J, Wang H, Mani A, Mani MA, Nelson-Williams C, Carew KS, Mane S, Najmabadi H, Wu D, et al. 2007. Lrp6 mutation in a family with early coronary disease and metabolic risk factors. Science. 315(5816):1278–1282.

Massink MP, Creton MA, Spanevello F, Fennis WM, Cune MS, Savelberg SM, Nijman IJ, Maurice MM, van den Boogaard MJ, van Haaften G. 2015. Loss-of-function mutations in the wnt co-receptor lrp6 cause autosomal-dominant oligodontia. Am J Hum Genet. 97(4):621–626.

Mattheeuws N, Dermaut L, Martens G. 2004. Has hypodontia increased in Caucasians during the 20th century? A meta-analysis. Eur J Orthod. 26(1):99–103.

Ockeloen CW, Khandelwal KD, Dreesen K, Ludwig KU, Sullivan R, van Rooij I, Thonissen M, Swinnen S, Phan M, Conte F, et al. 2016. Novel mutations in LRP6 highlight the role of wnt signaling in tooth agenesis. Genet Med. 18(11):1158–1162.

Prasad MK, Geoffroy V, Vicaire S, Jost B, Dumas M, Le Gras S, Switala M, Gasse B, Laugel-Haushalter V, Paschaki M, et al. 2016. A targeted next-generation sequencing assay for the molecular diagnosis of genetic disorders with orodental involvement. J Med Genet. 53(2):98–110.

Rakhshan V, Rakhshan A. 2016. Systematic review and meta-analysis of congenitally missing permanent dentition: sex dimorphism, occurrence patterns, associated factors and biasing factors. Int Orthod. 14(3):273–294.

Roslan Z, Muhamad M, Selvaratnam L, Ab-Rahim S. 2019. The roles of low-density lipoprotein receptor-related proteins 5, 6, and 8 in cancer: a review. J Oncol. 2019:4536302.

Ross J, Fennis W, de Leeuw N, Cune M, Willemze A, Rosenberg A, Ploos van Amstel HK, Creton M, van den Boogaard MJ. 2019. Concurrent manifestation of oligodontia and thrombocytopenia caused by a contiguous gene deletion in 12p13.2: a three-generation clinical report. Mol Genet Genomic Med. 7(6):e679.

Shi Z, Yang X, Li BB, Chen S, Yang L, Cheng L, Zhang T, Wang H, Zheng Y. 2018. Novel mutation of LRP6 identified in Chinese Han population links canonical WNT signaling to neural tube defects. Birth Defects Res. 110(1):63–71.

Singh R, Smith E, Fathzadeh M, Liu W, Go GW, Subrahmanyan L, Faramarzi S, McKenna W, Mani A. 2013. Rare nonconservative LRP6 mutations are associated with metabolic syndrome. Hum Mutat. 34(9):1221–1225.

Song S, Han D, Qu H, Gong Y, Wu H, Zhang X, Zhong N, Feng H. 2009. EDA gene mutations underlie non-syndromic oligodontia. J Dent Res. 88(2):126–131.

Song S, Zhao R, He H, Zhang J, Feng H, Lin L. 2014. WNT10A variants are associated with non-syndromic tooth agenesis in the general population. Hum Genet. 133(1):117–124.

Thesleff I, Sharpe P. 1997. Signalling networks regulating dental development. Mech Dev. 67(2):111–123.

van der Hout AH, Oudesluijs GG, Venema A, Verheij JB, Mol BG, Rump P, Brunner HG, Vos YJ, van Essen AJ. 2008. Mutation screening of the ectodysplasin—a receptor gene EDAR in hypohidrotic ectodermal dysplasia. Eur J Hum Genet. 16(6):673–679.

van Genderen C, Okamura RM, Farinas I, Quo RG, Parslow TG, Bruhn L, Grosschedl R. 1994. Development of several organs that require inductive epithelial-mesenchymal interactions is impaired in LEF-1-deficient mice. Genes Dev. 8(22):2691–2703.

Wang F, Flanagan J, Su N, Wang LC, Bui S, Nielson A, Wu X, Vo HT, Ma XJ, Luo Y. 2012. RNAscope: a novel in situ RNA analysis platform for formalin-fixed, paraffin-embedded tissues. J Mol Diagn. 14(1):22–29.

Williams BO, Insogna KL. 2009. Where Wnts went: the exploding field of Lrp5 and Lrp6 signaling in bone. J Bone Miner Res. 24(2):171–178.

Wong S, Liu H, Bai B, Chang H, Zhao H, Wang Y, Han D, Feng H. 2014. Novel missense mutations in the AXIN2 gene associated with non-syndromic oligodontia. Arch Oral Biol. 59(3):349–353.

Wong SW, Han D, Zhang H, Liu Y, Zhang X, Miao MZ, Wang Y, Zhao N, Zeng L, Bai B, et al. 2018. Nine novel PAX9 mutations and a distinct tooth agenesis genotype-phenotype. J Dent Res. 97(2):155–162.

Xu Y, Gong W, Peng J, Wang H, Huang J, Ding H, Wang DW. 2014. Functional analysis LRP6 novel mutations in patients with coronary artery disease. PLoS One. 9(1):e84345.

Yu M, Wong SW, Han D, Cai T. 2019. Genetic analysis: Wnt and other pathways in nonsyndromic tooth agenesis. Oral Dis. 25(3):646–651.

Yu M, Liu Y, Liu H, Wong SW, He H, Zhang X, Wang Y, Han D, Feng H. 2019. Distinct impacts of bi-allelic WNT10A mutations on the permanent and primary dentitions in odonto-onycho-dermal dysplasia. Am J Med Genet A. 179(1):57–64.

Yu M, Liu Y, Wang Y, Wong SW, Wu J, Liu H, Feng H, Han D. 2020. Epithelial WNT10A is essential for tooth root furcation morphogenesis. J Dent Res. 99(3):311–319.

Yu P, Yang W, Han D, Wang X, Guo S, Li J, Li F, Zhang X, Wong SW, Bai B, et al. 2016. Mutations in WNT10B are identified in individuals with oligodontia. Am J Hum Genet. 99(1):195–201.